J. metamorphic Geol. 1988, **6**, 235–254

A polycyclic two-stage corona growth in the Iforas Granulitic Unit (Mali)

A.-M. BOULLIER, *Centre de Recherches Pétrographiques et Géochimiques, B.P.20, F 54501 Vandoeuvre-les-Nancy Cedex, France*
P. BARBEY, *Universite de Nancy I, Laboratoire de Pétrologie, B.P. 239, F 54506 Vandoeuvre-les-Nancy Cedex, France and CRPG, B.P. 20, F54501 Vandoeuvre-les-Nancy Cedex, France*

Abstract. Retrograde and prograde mineral assemblages from metapelitic and metabasic rocks of the Iforas Granulitic Unit (Mali) were generated by the superimposition of two granulite facies metamorphic events. They clearly result from a polycyclic evolution and can be related to a late Eburnean unroofing followed by a Pan-African burial.

Thermobarometry on Pan-African garnet-bearing assemblages yields *(P,T)* estimates of 620±50°C and 5± 1kbar. The nearly anhydrous conditions produced in the Eburnean appear to be the direct cause of the unusually low-temperature granulite-facies metamorphism in the Pan-African. These *P,T* estimates are compared with those obtained on the underlying unit (Kidal Assemblage) upon which the Iforas Granulitic Unit was thrust. A *P–T–t* path, during the Pan-African orogeny, is proposed and discussed for both the Iforas Granulites and Kidal Assemblage.

Key-words: Eburnean orogeny; geothermobarometry; Pan-African orogeny; polymetamorphism; *P–T–t* path.

INTRODUCTION

Studies of disequilibrium metamorphic textures in structurally well-known metamorphic units are of particular interest because they give information of changing *P–T* conditions during the tectonic evolution of a crustal segment and consequently contribute to our understanding of the tectonic processes involved in the evolution of orogenic belts.

Garnet-forming reactions have frequently been observed in mafic assemblages (e.g. McLelland & Whitney, 1980; Bingen, Demaiffe & Delhal, 1984; Ellis & Green, 1985; Harley, 1985) but two-stage corona growth has rarely been described (Garde, Glassley & Nutman, 1984; Schenk, 1984). These two-stage coronas are considered to be monocyclic and arise either from short-lived fluctuations in a_{SiO_2} or P_{H_2O} at essentially constant *P* and *T* such as in Greenland (Garde *et al.*,1984) or from a unique *P–T–t* path such as during the Hercynian orogeny in Calabria (Schenk, 1984). However, it has been argued that the second stage coronas of these latter granulites may also better result from Alpine recrystallization (Vielzeuf,1984).

The retrograde and prograde mineral reactions we describe in the Iforas Granulitic Unit (Mali) clearly arise from a polycyclic evolution and can be related to a late-Eburnean unroofing followed by a Pan-African burial, leading to remarkable resorption and rim textures. An estimate of the *P,T* conditions during the Pan-African thrust tectonics event based on these textures has been attempted. We discuss the significance of the inferred *P–T–t* path and its bearing on the tectonic history of the unit during the Pan-African.

GEOLOGICAL SETTING

The Pan-African mobile belt of the Hoggar–Iforas region (Trans-Saharan belt, Cahen, Snelling, Delhal & Vail, 1984) is interpreted as the result of a collision between the passive margin of the West African craton and the active margin of the Tuareg shield (Fig.1a; Black, Caby, Moussine-Pouchkine, Bayer, Bertrand, Boullier, Fabre & Lespuer, 1979; Caby, Bertrand & Black, 1981). In this region, the Iforas Granulitic Unit (IGU) is a polycyclic unit

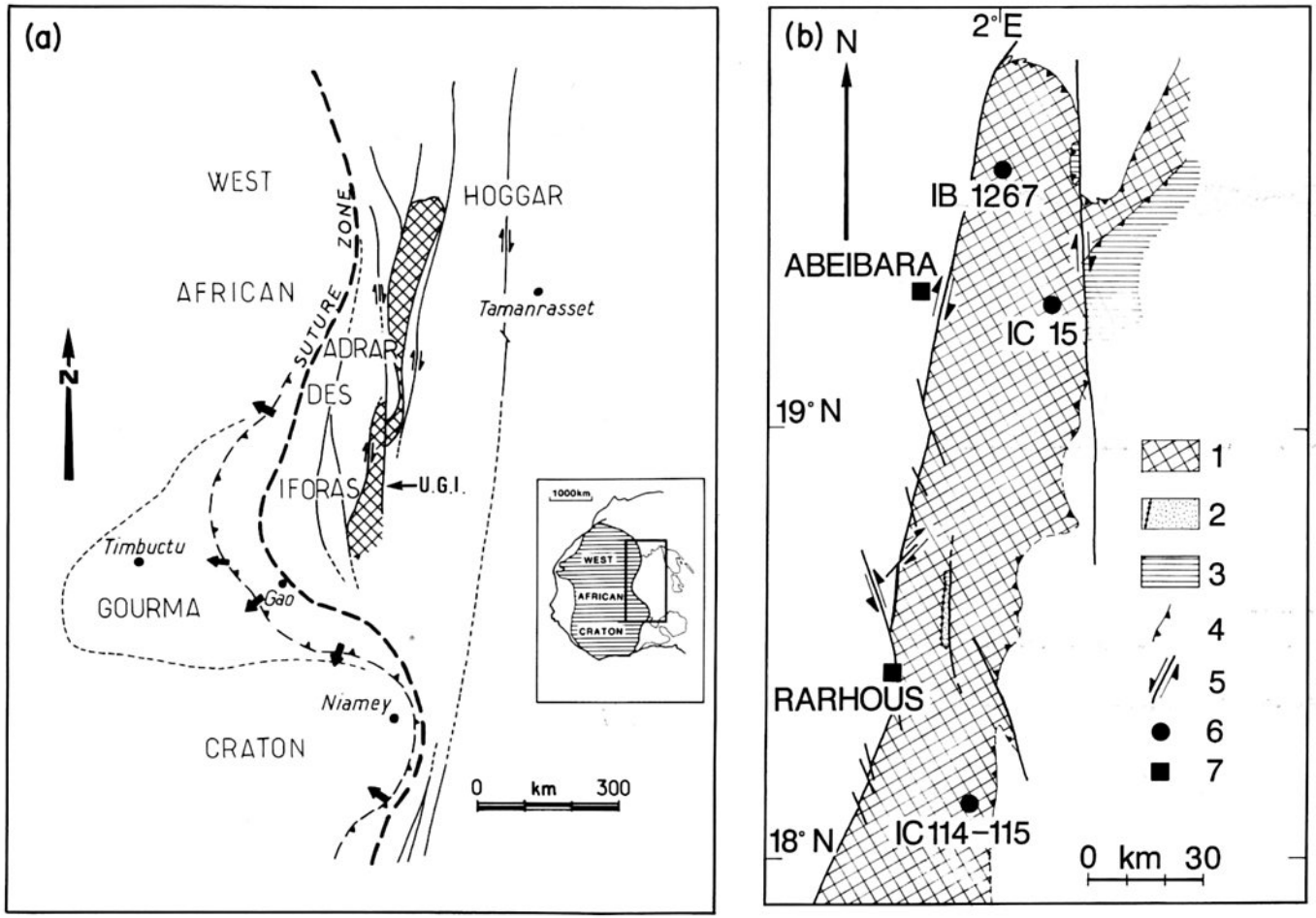

Fig. 1. Geological sketch maps for the Trans-Saharan fold belt in the Adrar des Iforas (a) and for the Iforas Granulitic Unit (b): (1) granulite facies rocks; (2) autochtonous Upper Proterozoic sedimentary cover; (3) allochthonous Upper Proterozoic sedimentary unit; (4) thrust plane; (5) strike–slip fault; (6) sampling localities; (7) well.

affected by a main Eburnean granulite facies metamorphic event and later involved as a nappe in the Pan-African orogeny (Boullier, Davison, Bertrand & Coward, 1978). The IGU is overthrust onto a migmatitic gneiss unit (Kidal Assemblage) and overlain through a sedimentary unconformity by an Upper Proterozoic low-grade metasedimentary cover. A third unit made of Upper Proterozoic supracrustals is thrust over the IGU (Fig. 1b). The IGU is composed of metasedimentary (metapelites, quartzites, rare marbles) and metaigneous rocks (ultramafic rocks, norites and charnockites) interspersed within a monotonous series of sub-alkaline quartzo-feldspathic gneisses of uncertain origin. Field relationships, petrography and structure have been detailed in several previous papers (Boullier *et al.*, 1978; Davison, 1980; Boullier, 1979, 1982; Bertrand, Michard, Carpena, Boullier, Dautel & Ploquin, 1984; Champenois, Boullier, Sautter, Wright & Barbey, 1987).

EVIDENCE FOR A POLYCYCLIC EVOLUTION

The IGU was first metamorphosed under granulite facies conditions and then retrogressed under low pressure – high temperature conditions, leading to widespread resorption textures. U/Pb data on zircons show that this main granulite facies metamorphic event occurred 2,120 ± 20Ma ago (Lancelot, Boullier, Maluski & Ducrot, 1983). After the Eburnean orogeny, the IGU outcropped at the peneplain level and was unconformably overlain by a sedimentary cover. This cover starts with arkosic microconglomerates composed of granulite detritus (e.g. mesoperthites, quartz with rutile needles) and is attributed to the Upper Proterozoic by comparison with other sedimentary sequences in the belt. Both the granulites and their cover were later involved in the Pan-African deformation and metamorphism.

The IGU has mylonitic contacts with the underlying gneissic Pan-African Kidal Assemblage (Fig.1b). The earliest mylonitic contact (North and East) is the result of thrust movement in a North – South direction (D_1) and has been subsequently folded by a D_2 deformation (Boullier, 1979; Davison, 1980). By contrast, the western contact corresponds to a late N–10° dextral D_3 shear zone dated at *c.* 550 Ma (Lancelot *et al.*, 1983; Boullier, 1986) The core of the IGU has also been affected by the Pan-African deformation as shown by shear zones (Bertrand *et al.*, 1984; Fig.2) and folding of the Upper Proterozoic metasedimentary cover. However, large blocks of granulites free of Pan-African deformation have been preserved.

The Pan-African metamorphism is clearly indicated by the recrystallization of the metasedimentary cover under low-grade conditions (400–500°C; Boullier, 1982), by the growth of hornblende instead of clinopyroxene in the mylonitic subalkaline gneisses of the IGU and by the recrystallization of pre-tectonic D_1 basic dykes which intrude both the IGU and its

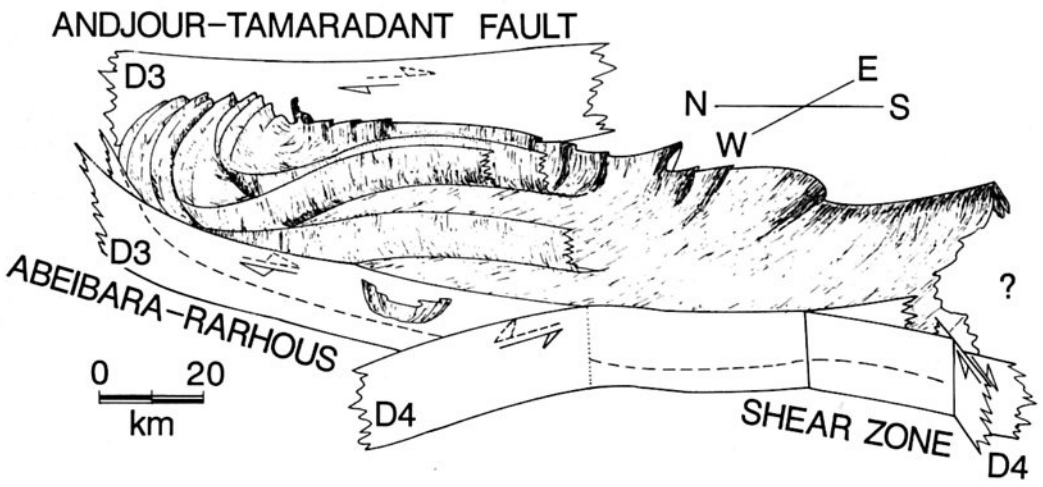

Fig. 2. Block diagram showing the geometry of the Iforas Granulitic Nappe (modified from Boullier, 1979).

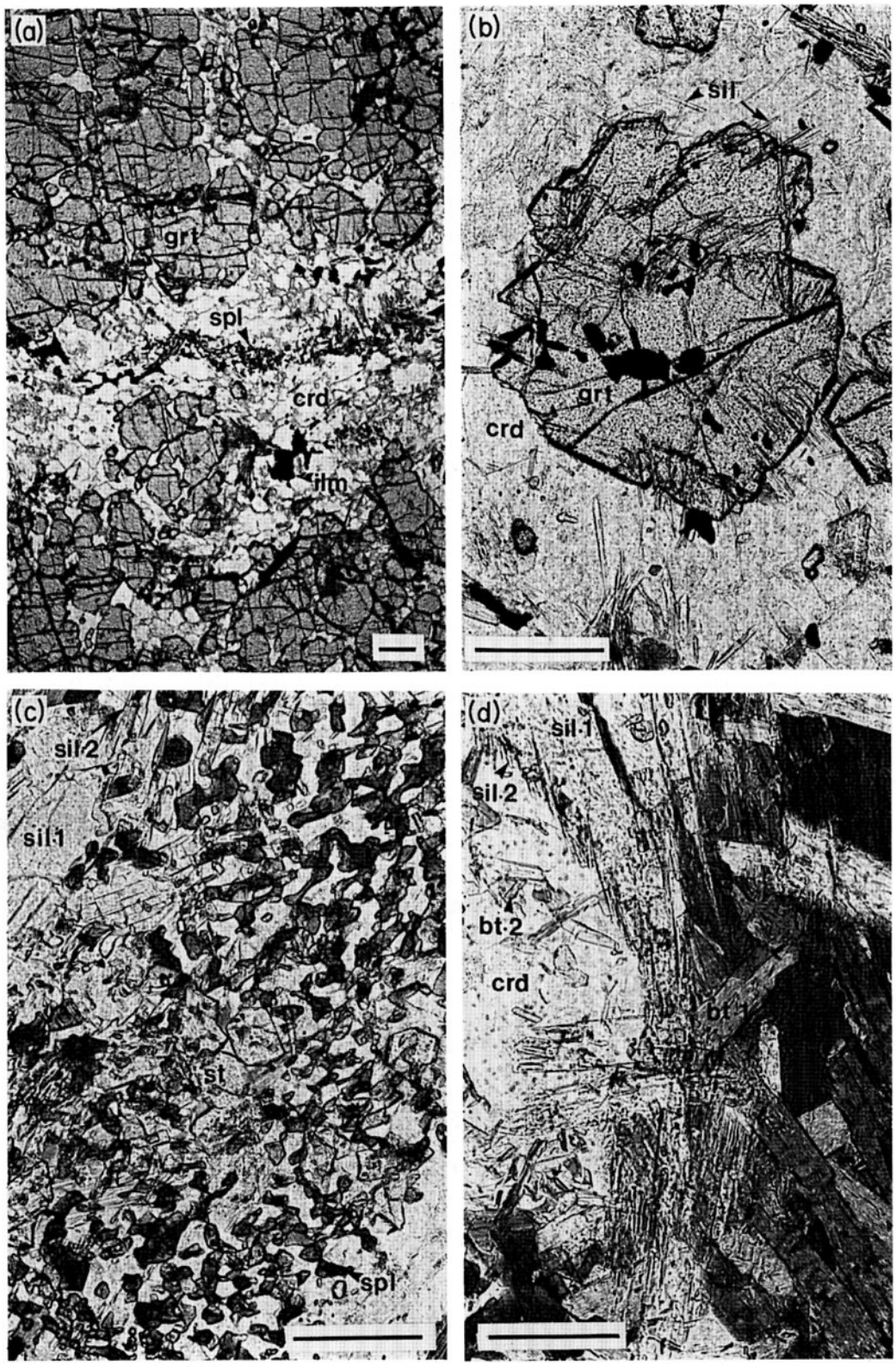
(a)
grt
spl
crd
ilm
(b)
sil
grt
crd
(c)
sil-2
sil-1
st
spl
(d)
sil-1
sil-2
bt-2
crd
bt

Upper Proterozoic metasedimentary cover. At the base of the IGU nappe, these basic dykes are transformed in amphibolites; garnet is present as well as biotite in subalkaline gneisses and prismatic sillimanite in aluminous mylonitic gneisses. However, all these metamorphic assemblages are deformed by the D_1 mylonitic event and sometimes by the D_2 event. Consequently, it is quite impossible to attribute any mineral to either the Eburnean or the Pan-African in the mylonitic base of the IGU.

Do the prograde garnet-bearing reaction rims in the IGU originate from this Pan-African metamorphic event? The most striking argument for the Pan-African age of these reaction rims is that some of the pretectonic D_1 basic dykes (Upper Proterozoic in age) display prograde garnet-bearing coronas similar to those found in the Iforas mafic granulites.

All the rocks studied, comprising metapelites and norites, were sampled near the base of the nappe as it can be reconstructed from the geometry of the deformation structures (Fig.1b and 2) and in regions either with abundant Pan-African gabbro and diorite bodies (samples IC–15 and IB–1267) or without intrusive rocks (IC–114, IC–115).

METAPELITES

The metapelitic granulites are aluminous migmatitic paragneisses and consist of alternating quartzo-feldspathic and alumina-rich, locally silica-undersaturated ferromagnesian layers. They display medium to coarse-grained granoblastic textures and are mainly composed of quartz, garnet, cordierite, sillimanite, graphite and more restricted amounts of alkali-feldspar, plagioclase, spinel and staurolite. Biotite forms layers in sample IB–1267, but is rare in IC–15.

Textures and mineral reactions

Three metamorphic stages have been recorded. The first two are Eburnean in age, the third Pan-African (Table 3 and Fig.6).

The oldest assemblage corresponding to the *Eburnean peak* metamorphic conditions, consists of GrtI + Kfs + Qtz + Pl + Sil + Rt + Gr. Pelitic gneisses suffered incipient partial melting and this assemblage was then retrogressed.

In sample IC–15, garnet porphyroblasts have been partly resorbed, locally fragmented (Fig.3a) and surrounded either by cordierite or cordierite + hercynite symplectitic assemblages. In silica-undersaturated layers containing garnet and sillimanite we observe the growth of cordierite toward garnet and of cordierite–hercynite symplectites toward sillimanite. These textures can be accounted for by the following two reactions:

$$\text{Grt} + \text{Sil} + \text{Qtz} \rightarrow \text{Crd}, \quad (1)$$

$$\text{Grt} + \text{Sil} \rightarrow \text{Crd} + \text{Hc} + \text{Pl}. \quad (2)$$

In Sample IB–1267 garnet and sillimanite are partly replaced by cordierite, itself rimmed by aggregates of brown-red biotite flakes with or without quartz and sillimanite (Fig.3d).

The *Pan-African* metamorphism led to the formation of several reaction rims and to the recrystallization of all the large Eburnean cordierite crystals into granoblastic aggregates of small grains (0.05–0.15mm).

The most widespread reaction corresponds to the growth of both garnet and sillimanite at the expense of cordierite corresponding to a displacement toward the left in the reaction (1). The smallest relict garnet grains (<0.2mm) enclosed in cordierite crystals (resulting from the Eburnean retrograde stage) recrystallized into euhedral crystals with radial sillimanite needles, forming sea-urchin-like textures (Fig.3b). Most larger garnets remain generally anhedral to subhedral (Fig. 3a).

The second type of reaction consists in the development of staurolite mainly at the expense of cordierite and sillimanite. The small euhedral staurolite crystals (<0.5mm), locally enclosing quartz blebs, grow preferentially close to or in the immediate vicinity of hercynite (Fig.3c) or around ilmenite and magnetite grains. However, textural relationships clearly show that staurolite developed from four main reactions (see Richardson, 1968) which are dependent upon the mineral assemblages:

$$\text{Crd} + \text{Hc}_{ss} \rightarrow \text{St} + \text{GrtII} \quad (3)$$

$$\text{Crd} + \text{Hc}_{ss} + \text{Sil} \rightarrow \text{St} \quad (4)$$

$$\text{Crd} + \text{Sil} \rightarrow \text{St} + \text{Qtz} \quad (5)$$

$$\text{Crd} + \text{Mag} + \text{Sil} \rightarrow \text{St} + \text{Qtz} \quad (6)$$

Small clusters of euhedral biotite flakes and sillimanite developed from cordierite (sample IB–1267; Fig.3d).

The non-systematic occurrence of all these reactions and especially the growth of garnet only from

Fig. 3. Resorption and rim textures in metapelites. Scale bar = 0.2mm. (a) Garnet porphyroblasts partly resorbed into cordierite and spinel, during the Eburnean retrograde stage (sample IC-15); (b) Pan-African euhedral garnet with radial sillimanite needles, within cordierite (sample IC-15); (c) Pan-African staurolite crystals grown from cordierite and spinel; Eburnean prismatic (sil-1) and Pan-African fibrolitic (sil-2) sillimanite crystals are also visible at the top left (sample IC-15); (d) Large rim of Eburnean brown biotite (bt-1) around cordierite and small Pan-African biotite flakes (bt-2) within cordierite (sample IB-1267).

Table 1. Representative analyses of minerals from the two studied metapelites

Sample	IC–15									IB–1267						
Mineral	Grt Rim 33 Euhedral	Grt Core 35 Euhedral	Crd 19	Grt Core 54 Anhedral	Crd 48	Grt Rim 56 Anhedral	Crd 57	Crd 35	Crd 36	Grt Core 5 Euhedral	Bt 1	St 34	Grt Core 8 Anhedral	Grt Rim 9 Anhedral	Crd Rim 10	Crd Core 12
SiO_2	38.08	38.45	48.84	37.78	48.2	37.65	48.31	49.19		37.94	34.48	26.59	38.6	38.35	48.37	49
TiO_2				0.01							1.18	0.26	0.04			
Al_2O_3	21.54	22.03	33.36	21.44	32.62	21.65	33	33.03	59.45	21.85	19.66	55.92	21.86	21.82	32.95	33.16
FeO	33.65	36.01	7.39	35.8	8.27	34.36	7.17	7.53	34.28	36.24	21.23	13.45	35.46	36.8	8.26	7.95
MnO	0.16	0.21	0.09	0.46		0.13		0.03		0.06		0.1	0.64	0.75		0.13
MgO	3.86	4.03	8.45	4.31	8.24	4.45	8.52	8.91	3.22	3.97	9.68	1.28	3.83	3.4	7.96	8.06
CaO	1.44	1.17	0.02	1.17	0.06	1.92	0.02	0.08		1.76	0.01		1.32	1.25	0.04	
Na_2O			0.11		0.18		0.18			0.05	0.29	0.04	0.04	0.01	0.14	0.03
K_2O											8.52	0.08				
ZnO							0.03		1.23			0.06				
Cr_2O_3									0.68							
Total	98.73	101.9	98.26	100.97	97.57	100.16	97.23	98.77	98.86	101.87	95.05	97.48	101.79	102.38	97.72	98.33
Oxygens	24	24	18	24	18	24	18	18	32	24	22	48	24	24	18	18
Si	6.108	6.023	5.004	5.995	5.002	5.994	5.007	5.033		5.969	5.291	7.405	6.105	6.017	5.008	5.03
Al^{iv}				0.005		0.006				0.031	2.709	0.595				
Al^{vi}	4.059	4.06	4.021	3.991	3.982	4.041	4.024	3.952	15.983	4.011	0.841	17.725	4.064	4.03	4.014	4.005
Ti											0.136	0.054	0.09			
Cr									0.123							
Fe	4.492	4.699	0.619	4.729	0.715	4.553	0.631	0.638	6.539	4.751	2.715	3.121	4.681	4.811	0.713	0.68
Mn	0.019	0.028		0.057		0.019	0.08			0.009		0.024	0.009	0.104		0.011
Mg	0.933	0.949	1.324	1.028	1.283	1.059	1.3	1.359	1.095	0.935	2.228	0.535	0.912	0.8	1.236	1.241
Ca	0.25	0.197		0.2	0.007	0.325		0.009		0.293			0.228	0.207		
Na			0.018		0.018		0.011				0.086		0.009		0.028	
K											1.669					
Zn									0.207							
OH												1.977				

small pre-existing grains suggest that these reactions are closely controlled by kinetic factors and correspond to local equilibria.

Secondary fluid inclusions are numerous in quartz crystals, but have not been observed in other minerals (garnet, cordierite, staurolite). Hence, it is impossible to attribute these inclusions to one precise stage of metamorphism (Eburnean or Pan-African). As a result, no detailed microthermometry has been performed. Observations show that only CO_2 and $CO_2 + H_2O$ ($X_{H_2O} \leq 0.1$ volume) inclusions are present. CO_2 is either monophase (liquid) or biphase (liquid + vapour) at room temperature. Inclusion shape is irregular suggesting decrepitation of early (Eburnean?) inclusions or incomplete healing of late (Pan-African?) microfractures. Whatever their age, these fluid inclusions suggest that P_{H_2O} remained low during the entire metamorphic history.

Mineral chemistry

Mineral compositions (Table 1) were determined with an automatized CAMEBAX electron microprobe at the Department of Microanalysis (University of Nancy I) operating at 15 KV, 10nA and using the MBXCOR correction procedure (Henoc & Tong, 1978).

Garnets are almandine–pyrope solid–solutions (X_{Fe} = 0.75–0.81; X_{Mg} = 0.13–0.18) with minor spessartine ($X_{Mn} < 0.02$) and grossular ($X_{Ca} < 0.05$) components. Garnet crystals show more or less complex zoning profiles. However, some constant patterns can be drawn from systematic measurements. The profiles of the small euhedral garnets (Fig. 3b) are characterized, from core to rim, by a decrease in X_{Fe} and rather constant or slightly increasing X_{Mg} and X_{Ca} (Fig.4 and Table 4), whereas those of the large subhedral to xenomorphic garnets display an increase in X_{Fe} rimward (Table 4). However, some discrepancies can be observed. More particularly, garnet X_{Fe} is dependent upon the neighbouring minerals and can increase significantly close to ilmenite grains.

Cordierite composition is rather constant as indicated by average composition and related standard deviation (X_{Fe} = 0.34 ± 0.02). The total fluid content average is 2.00 ± 0.75 wt%.

Staurolites have X_{Fe} (Fe/Fe+Mg+Mn) ranging from 0.81 to 0.87 with the lowest values when staurolite is associated with hercynite. The Zn content was always below the detection limit (<0.5 wt%) Spinels are mostly hercynite (X_{Fe} = 0.83–0.90) with low Mg-spinel (X_{Mg} = 0.10–0.15) and minor gahnite (X_{Zn} =0.03) components. Oxides are almost pure ilmenite (X_{Ilm} = 0.97–1.00, X_{Hem} = 0 – 0.02, X_{Gei} = 0 – 0.02). Plagioclase crystals are andesine (X_{An} = 0.45–0.50) apart from small grains with very high An contents (X_{An} = 0.88–0.94) observed in spinel –cordierite–staurolite aggregates. The presence of these An-rich plagioclases can be related to reaction (2) as shown by Vielzeuf (1984). No systematic zoning was observed.

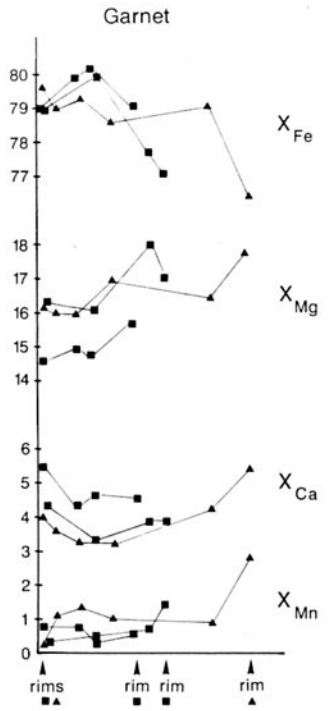

Fig. 4. Zoning profiles of small euhedral garnets (■) and of a large xenomorphic garnet (▲) from the metapelite IC-15. See also Table 4.

NORITES

Three samples comprising a norite (IC-115), an olivine–clinopyroxene–norite (IC-115B) and a phlogopite–norite (IC-114), were studies. They were all sampled from the same outcrop located near the southeastern border of the IGU in an area free from Pan-African intrusive rocks (Fig.1b). These three rock types are tectonically concordant with the regional Eburnean metamorphic layering and are associated with spinel-pyroxenites and metapelites. The spinel-pyroxenites which do not show any reaction linked to the Pan-African metamorphism, will not be described in this section.

Textures and mineral reactions

Norite IC-115

The primary texture of this rock is coarse-grained equigranular granoblastic. The mineral assemblage belonging to the *Eburnean peak* metamorphic conditions may be reconstituted as follows: GrtI+

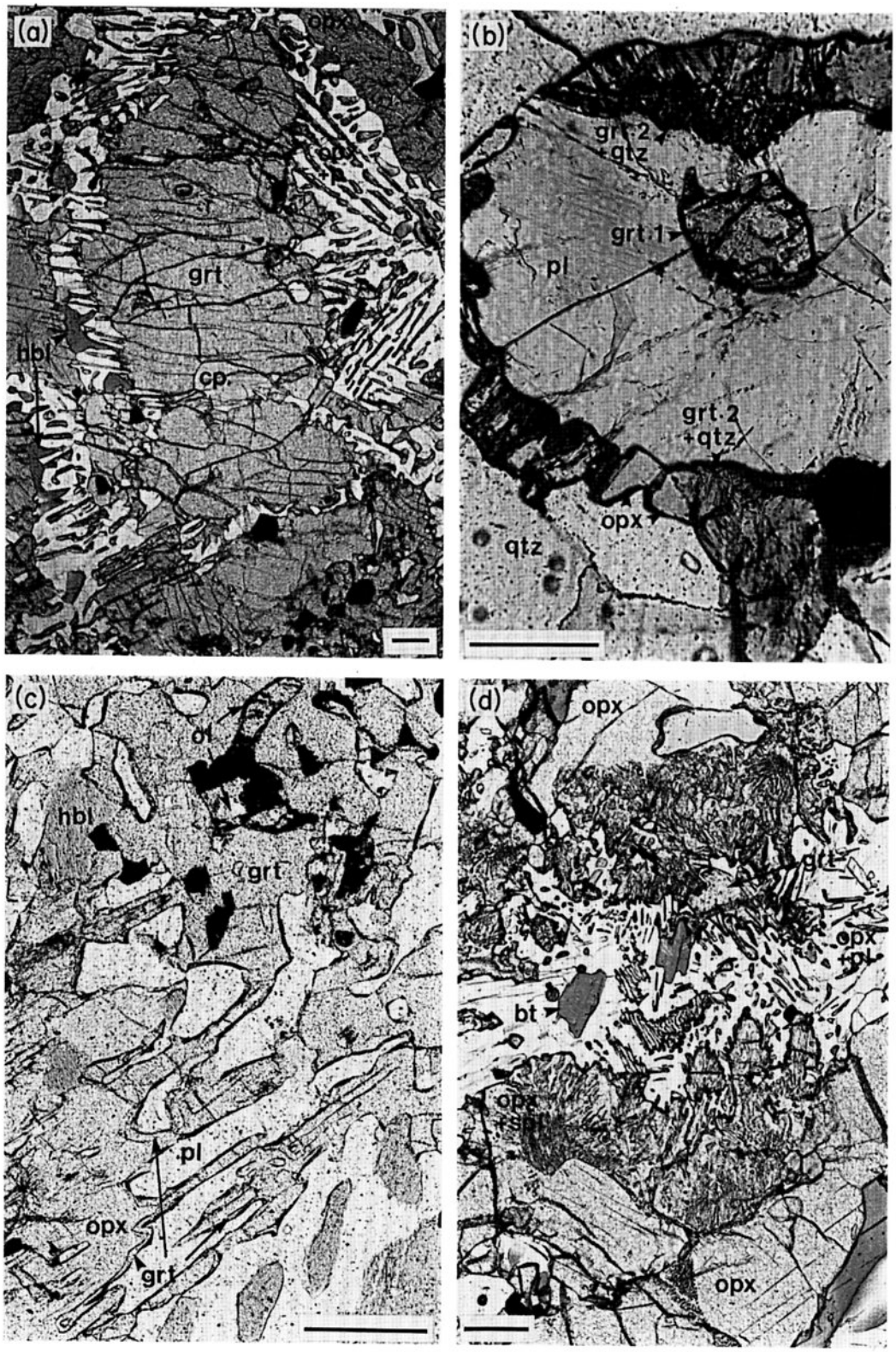
(a)
opx
grt
hbl
cp.
(b)
grt 2
+qtz
grt 1
pl
grt 2
+qtz
opx
qtz
(c)
ol
hbl
grt
pl
opx
grt
(d)
opx
grt
opx
+pl
bt
opx
+spl
opx

OpxI+CpxI+Pl+Qtz+Ilm. Primary garnets are rare and are observed only in a few cases (Fig.5b). Orthopyroxene is characterized by clinopyroxene exsolution lamellae along cleavages and primary plagioclase contains antiperthite preserved in the core of the crystals.

The retrograde granulitic Eburnean stage led to the breakdown of garnet I and quartz into symplectitic assemblages of orthopyroxene II and plagioclase II, according to the reaction:

$$GrtI + Qtz \rightarrow OpxII + PlII. \quad (7)$$

This reaction led to the development of typical patchy textures. The patches (2–4mm) are composed of a corona of coarse-grained granoblastic orthopyroxene II free of clinopyroxene exsolution lamellae, surrounding a core consisting of a symplectitic assemblage of plagioclase II containing orthopyroxene II vermicules (see for instance Fig.5a). These orthopyroxene vermicules are sometimes in crystallographic continuity with the large corona orthopyroxenes. Orthopyroxene and ilmenite are occasionally fringed with a narrow band of greenish-brown hornblende. In some cases, orthopyroxene I recrystallized and exsolution lamellae or blebs of clinopyroxene have coalesced to give large bands alternating with the recrystallized orthopyroxene. In other cases, blebs of orthopyroxene and clinopyroxene are included in plagioclase II. Plagioclase II does not contain antiperthite but is often slightly zoned with a more An-rich margin. This zoning could occur during decompression as a result of a reaction such as

$$Cpx + PlI \rightarrow Opx + PlII \quad (8)$$

The *Pan-African* metamorphism led to the local growth of garnet II between plagioclase and orthopyroxene (Fig.5c and 6) through the reverse reaction of reaction (7) and between ilmenite and plagioclase according to the reaction:

$$Ilm + Pl \rightarrow Grt + Qtz. \quad (9)$$

Secondary garnets contain abundant quartz blebs mostly visible in the large crystals. Orthopyroxene remains stable with quartz therefore suggesting that Pan-African recrystallization also occurred under granulite facies conditions.

As in the metapelite IC-15, fluid inclusions are present in quartz crystals only and are impossible to relate to any precise stage of the metamorphic history. Three main types of fluid inclusion have been observed: (1) irregular CO_2 liquid fluid inclusion; (2) NaCl brines; (3) H_2O and CO_2 (liquid or liquid + vapour at room temperature), and sometimes salt; this type of fluid inclusions could result from the mixing of the other two.

Olivine–clinopyroxene–norite IC-115B

The whole metamorphic evolution of this sample is similar to that of the previously described norite IC-115, except for the presence of olivine leading to an additional garnet-forming reaction (Table 3 and Fig. 5c and 6). The *Eburnean* highest grade assemblage is composed of garnet, orthopyroxene, clinopyroxene, minor plagioclase and ilmenite. It is difficult to ascertain whether olivine belongs to this assemblage. Both ortho- and clinopyroxene contain exsolution lamellae along cleavages. Olivine occurs as aggregates of small grains (<0.2 mm) often surrounded by orthopyroxene.

The first assemblage was retrogressed into a symplectitic association of plagioclase and orthopyroxene (± brown hornblende) vermicules (Fig.5a) according to the reaction:

$$Grt + Cpx \rightarrow Opx + Pl + Qtz. \quad (10)$$

Plagioclase frequently encloses small grains of olivine suggesting that the olivine–plagioclase assemblage was stable at the end of the Eburnean metamorphism.

As in the previous sample the *Pan-African* metamorphic event led to the growth of a late generation of garnet between plagioclase and orthopyroxene (reaction (7)) or plagioclase and olivine (Fig.5c) according to the reaction:

$$Ol + Pl \rightarrow Grt. \quad (11)$$

Phlogopite–Norite IC-114

The primary assemblage can be approximately reconstructed as consisting of orthopyroxene containing tiny needles of rutile in a 3-D lattice, garnet and minor plagioclase.

During the *Eburnean* retrograde stage, this early assemblage was destabilized through complex reactions leading to corona textures and to the growth of large mica flakes outlining a weak foliation. The coronas consist of a core of plagioclase grains in symplectitic association with orthopyroxene and spinel vermicules, surrounded by granoblastic aggregates of coarse-grained orthopyroxene which contains abundant spinel vermicules close to the plagioclase contact (Fig. 5d). The spinel vermicules sometimes coalesce and give larger grains or strings along grain

Fig. 5. Resorption and rim textures in norites. Scale bar = 0.2mm. (a) Garnet porphyroblast partly resorbed into a symplectite of orthopyroxene and plagioclase with minor brown hornblende, during the Eburnean retrograde stage (sample IC-115B); (b) Two-stage corona texture: relict Eburnean garnet grain (grt-1) destabilized into plagioclase and orthopyroxene, and Pan-African garnet–quartz rim (grt-2) between orthopyroxene and plagioclase (sample IC-115); (c) Pan-African garnet rims around orthopyroxene, brown hornblende and olivine (sample IC-115B); (d) Pan-African garnet developed on a former orthopyroxene-plagioclase symplectite; note the orthopyroxene-spinel symplectite formed according to reaction (12) during the Eburnean retrograde stage (sample IC-114A).

Table 2. Representative analyses of Grt–Ol–Pl and Grt–Opx–Pl triplets from the three studied norite samples. Structural formulae of olivine, garnet, orthopyroxene and plagioclase on the basis of 4, 12, 6 and 8 oxygens respectively

Sample	IC–115B						IC–115			IC–114A		
	01	Grt	Pl	Opx	Grt	Pl	Opx	Grt	Pl	Opx	Grt	Pl
SiO_2	34.54	39.09	46.17	52.00	39.33	46.35	48.95	38.64	55.39	50.09	40.20	59.05
Al_2O_3	0.03	21.97	35.04	1.87	21.99	34.58	0.92	21.00	29.02	7.40	23.83	25.27
FeO	44.47	26.01	0.09	24.89	25.08	0.16	38.97	29.21	0.32	17.14	24.29	0.11
MnO	0.45	1.79		0.56	1.65		0.60	1.47		0.19	1.02	
MgO	19.12	5.29		19.41	4.97		9.37	1.77		24.15	12.12	
CaO	0.04	6.67	18.29	0.72	6.94	17.51	0.56	8.58	11.51		1.01	6.29
Na_2O	0.07		1.12		0.03	1.33			4.95			7.95
K_2O	0.03		0.04						0.30			0.12
TiO_2				0.09	0.10	0.02	0.08			0.11		
Total	98.75	100.82	100.75	99.57	100.09	99.95	99.45	100.67	101.49	99.08	102.47	98.79
Si	1.021	3.019	2.110	1.969	3.046	2.131	1.994	3.046	2.466	0.832	2.961	2.663
Al^{IV}			1.887	0.031		1.874	0.006		1.523	0.168	0.039	1.343
Al^{VI}	0.001	2.000		0.052	2.007		0.038	1.951	0.012	0.151	2.031	0.004
Ti		0.001		0.003	0.006		0.002			0.003		
Mg	0.843	0.609		1.096	0.574		0.569	0.208		1.317	1.331	
Fe	1.100	1.680	0.003	0.788	1.624	0.006	1.327	1.877		0.524	1.496	
Mn	0.011	0.117		0.018	0.108		0.021	0.098		0.006	0.064	
Ca		0.552	0.896	0.029	0.576	0.863	0.024	0.725	0.549		0.079	0.304
Na			0.099			0.119			0.427			0.695
K			0.002						0.017			0.007

boundaries. This could be part of the exsolved MgTs component:

$$MgAl_2SiO_6 = MgAl_2SiO_2 + SiO_2 . \quad (12)$$

Orthopyroxenes have rectilinear or curvilinear grain boundaries with 120° triple junctions and show straight kink-band boundaries normal to (100). Relationships between neighbouring crystals suggest that some grains come from a single large crystal by syntectonic recrystallization or the evolution of kink-band boundaries into grain boundaries.

In a subsequent stage, garnet formed from orthopyroxene and plagioclase, or from biotite and plagioclase (Fig.5d). As in the previous samples, this prograde reaction is interpreted as *Pan-African* in age.

Mineral chemistry (Table 2)

Norite IC-115

Garnets display systematic chemical variations between the cores of primary relict garnet and secondary garnet rims growing from plagioclase and orthopyroxene. The cores of large primary garnets have the highest X_{Mg} and the lowest X_{Ca} values ($X_{Mg} \geq 0.09$; $X_{Ca} \leq 0.19$) whereas the rims have intermediate values ($X_{Mg} \leq 0.08$; $X_{Ca} \geq 0.20$) similar to those of the small relict primary garnets. Secondary garnets have X_{Mg} contents in the range 0.05–0.07 and X_{Ca} in the range 0.21–0.26 (average 0.24 ± 0.01).

There are no significant compositional variations between the cores and the rims of the large orthopyroxene crystals and the vermicules included in the plagioclase. Their compositions vary over a narrow range (X_{Fe} = 0.65–0.70, X_{Mg} = 0.29–0.32, and X_{Ca} = 0.01–0.02) and they are characterized by a low Al_2O_3 content (<1 wt%). Exsolved clinopyroxene in orthopyroxene and vermicules of clinopyroxene in plagioclase are in the same compositional range (X_{Mg} = 0.23–0.26).

Secondary antiperthite-free plagioclases have higher X_{An} (range 0.54–0.75, average 0.62±0.06) than primary plagioclase (range 0.48–0.60, average 0.53±0.04) which is characterized by the presence of antiperthite (X_{Or} = 0.93–0.97, X_{Ab} = 0.03–0.07, X_{An} = 0–0.01). With the exception of a few hematite grains, oxides are essentially ilmenite (X_{Ilm} = 0.89–0.95, X_{Hem} = 0.01–0.05).

Olivine-clinopyroxene norite IC-115B

Relict Eburnean garnets have X_{Mg} ranging from 0.24 to 0.26 whereas small Pan-African garnets which occur as rims around olivine and orthopyroxene crystals, have lower X_{Mg} (0.21–0.17). In all types of garnet X_{Ca} remains almost constant (0.18–0.21).

The composition of both the large orthopyroxene crystals and the vermicules included in plagioclase lies in a restricted range (X_{Fe} = 0.39–0.45). Only the small orthopyroxenes forming rims around olivines have lower X_{Fe} (around 0.31). Al_2O_3 contents are in all cases low (≤ 1.8 wt%). The composition of clinopyroxene is also rather constant (X_{Mg} = 0.34–0.38, X_{Ca} = 0.39–0.47).

Olivine is characterized by a quite restricted compositional range (X_{Fo} = 0.41–0.43) irrespective of its association with garnet or othopyroxene.

Plagioclase is a bytownite (X_{An} = 0.86–0.90) and does not show systematic variation around corona textures. Oxides are mainly ilmenite (X_{Ilm} = 0.96–0.99, X_{Hem} = 0.02–0.04) with a few grains of hematite (X_{Hem} = 0.98–1, X_{Ilm} = 0–0.02).

Phlogopite–norite IC-114

Primary garnets display weak zoning with more Mg-rich cores (range X_{Mg} = 0.46–0.50, average 0.48±0.01) than rims (range X_{Mg} = 0.45–0.48, average 0.47±0.01). Secondary garnets which have grown from orthopyroxene and plagioclase have significantly lower X_{Mg} ($0.43 < X_{Mg} < 0.46$, average 0.45±0.01). Secondary garnets growing at the expense of biotite have still lower X_{Mg} ($0.38 < X_{Mg} < 0.43$, average 0.40±0.02). The X_{Ca} (0.02) and X_{Mn} (0.01) contents remain low and do not show significant variations.

For all types of orthopyroxenes X_{Mg} varies in the range 0.69–0.73. Spinel vermicules and grains in both orthopyroxene and plagioclase are hercynite-Mg spinel solid solutions (X_{Fe} = 0.42–0.52). Biotite does not show significant compositional zoning (X_{Mg} = 0.87±0.02).

Primary plagioclases are oligoclases (X_{An} = 0.28–0.29) whereas secondary plagioclases are andesine (X_{An} = 0.30–0.34) with slightly more An-rich margins.

ESTIMATION OF *P,T* CONDITIONS

The main successive mineral reactions (summarized in Table 3 and on Fig.6) and field relationship indicate that the granulites were decompressed at the end of the Eburnean orogeny and then buried again during the Pan-African event. Most of garnet forming reactions observed in both metapelitic and mafic rocks have been calibrated as geobarometers or geothermometers and can be used to estimate the *P,T* conditions prevailing the IGU during the Pan-African. These *P,T* estimates have been performed only from new garnet grains and rims of older minerals which can be, *a priori*, considered as representative of the Pan-African metamorphic event. A full set of data for these *P,T* calculations is available from the senior author on request. A *P,T* estimate from fluid inclusions has not been attempted because, as outlined before, there are no reliable criteria to distinguish among the several generations of fluid inclusions.

Table 3. Summary of the main successive mineral assemblages and reactions during the Eburnean (E1 and E2) and Pan-African (PA) metamorphic events. See related textures in Fig. 6. A negative number in the reaction column indicates that the reaction as given in the text is reversed.

Sample number	Mineral assemblages	Reactions	
IC–15 and IB–1267	(E1) Grt+Sil+Qtz+Kfs+Pl+Rt+Gr+Ilm		
		Grt+Sil+Qtz→Crd	(1)
		Grt+Sil→Crd+Hc+Pl	(2)
	(E2) Crd+GrtI+Sil+Qtz+Kfs+Pl+Bt+Gr+Rt+Ilm		
		Crd→Grt+Sil+Qtz	(−1)
		Crd+Hc→St+Grt	(3)
		Crd+Hc+Sil→St	(4)
		Crd+Sil→St+Qtz	(5)
		Crd+Mag+Sil→St+Qtz	(6)
	(PA) GrtI+GrtII+Crd+Sil+St+Qtz+Kfs+Pl+Hc+Bt+Gr+Rt+Ilm		
IC–115	(E1) Grt+OpxI+CpxI+Pl I+Qtz+Ilm		
		Grt+Qtz→Opx+Pl	(7)
		Cpx+PlI→Opx+PlII	(8)
		Grt+Cpx→Opx+PlII+Qtz	(10)
	(E2) GrtI+OpxI+OpxII+CpxI+PlII+Qtz+Hbl+Ilm		
		Opx+Pl→Grt+Qtz	(−7)
		Ilm+Pl→Grt+Qtz	(9)
	(PA) GrtI+GrtII+OpxI+OpxII+CpxI+PlII+Hbl+Ilm		
IC–115B and IC–114A	(E1) GrtI+OpxI+Cpx+Pl+Ilm	Grt+Qtz→Opx+Pl	(7)
		MgTs→Spl+Qtz	(12)
	(E2) GrtI+OpxI+OpxII+Cpx+Pl+Ol+Ilm		
		Opx+Pl→Grt+Qtz	(−7)
		Ol+Pl→Grt	(11)
		Ilm+Pl→Grt+Qtz	(9)
	(PA) GrtI+GrtII+OpxI+OpxII+CpxI+Pl+Ol+Ilm		

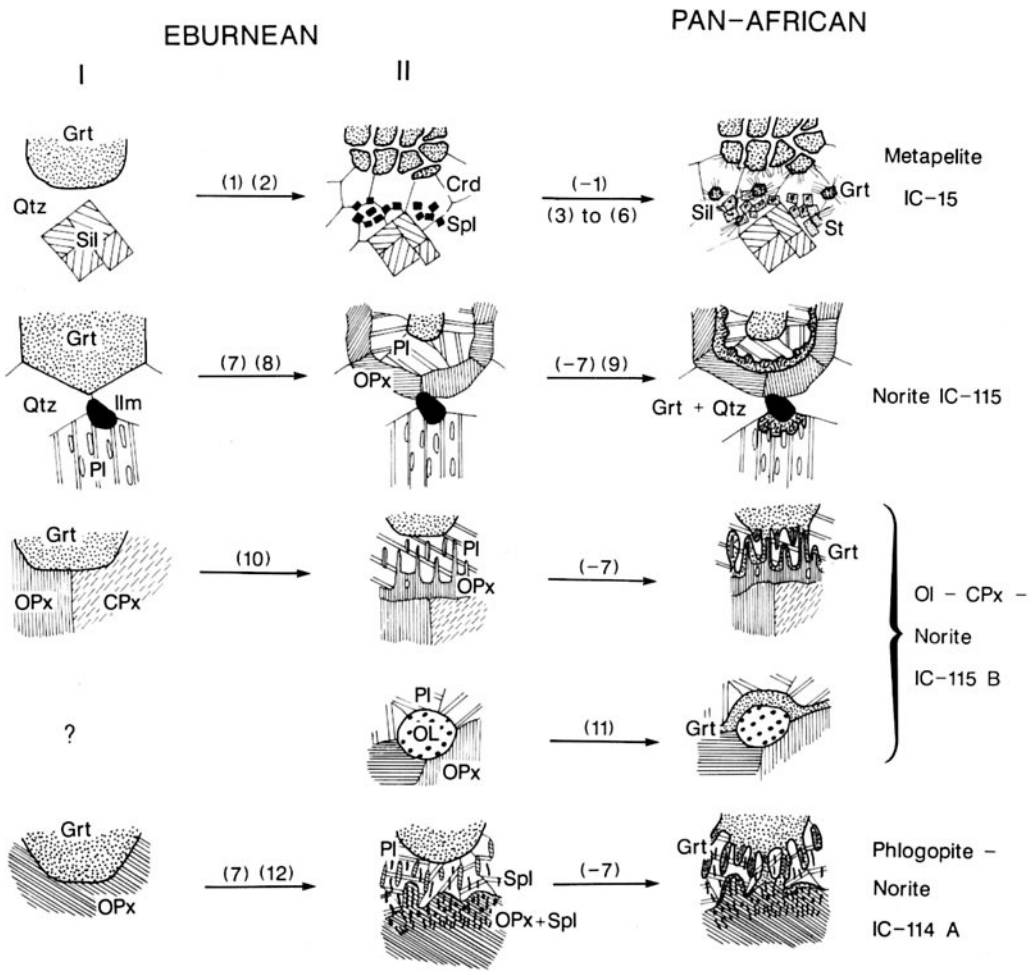

Fig. 6. Synthetic diagram for the main Eburnean and Pan-African mineral reactions and related textures in metapelites and norites. Numbers between brackets refer to the reactions given in the text and in Table 3.

Thermobarometry on metapelitic assemblages

Temperatures

Temperatures were estimated from Crd–Grt, Crd–Spl and Grt–Bt assemblages. All the thermometric expressions based on these assemblages assume ideal mixing of garnet components.

Temperatures calculated from Grt–Crd assemblages with the calibrations of Thompson (1976) are in the range 572–627°C for sample IB-1267 and in the range 545–658°C for sample IC-15 (Fig.7a). Estimates from small euhedral garnets and from rims of larger garnets are identical. Temperatures obtained from the calibrations of Wells (1979) and Martignole & Sissi (1981) fall in the same range (520–635°C and 510–640°C, respectively).

The Fe–Mg exchange equilibrium between cordierite and spinel has also been used for thermometric purposes (Vielzeuf, 1983). This thermometer yields results (517–656°C) in the same range as the Crd–Grt thermometer (Fig.7b).

Temperatures obtained from two Grt–Bt pairs using the calibration of Ferry & Spear (1978) and Hodges & Spear (1982) (576–671°C and 530–624°C, respectively) are consistent

with the above estimates, whereas temperatures given by the calibration of Pigage & Greenwood (1979) are rather high (621–708°C).

The Zn content of spinel in Bt–Sil–Spl assemblages could not be used as a thermometer because of the silica-undersaturated chemistry of the alumina-rich layers in the metapelites (Montel, Weber & Pichavant, 1986).

The various temperature estimates are consistent with each other and indicate that the temperature of metamorphism is likely to have been in the range 550–650°C. It must be stressed that these temperatures are too low for Grt–Crd–Sil–Qtz assemblages to be stable at the relevant pressure of 4–5 kbar (see below) for $P_{H_2O} = P_{total}$. For instance, the relevant stability field, bounded by the curves labelled Bt–Sil–Qtz and FeCrd (see Fig.7 of Holdaway & Lee, 1977) extends down to 670°C at $P =$ 4 kbar for $P_{H_2O} = 0.4P_{total}$.

Therefore, the stability of the Grt–Crd–Sil–Qtz assemblage at these low temperatures (550–650°C) suggests strongly reduced water fugacity or, possibly, inappropriate calibration of the thermometric expressions (especially regarding modelling of the activity–composition relation of garnet). Nevertheless, the consistency of temperature estimates in metapelitic and in mafic assemblages (for which the non-ideal mixing of garnet components have been taken into account) together with the stability of the Opx–Qtz assemblage, the scarcity of biotite and the abundance of CO_2-rich fluid inclusions support the first hypothesis.

Pressures

Pressures estimated from the fluid dependent equilibrium Crd + Grt + Sil + Qtz must be regarded with caution because water fugacity is poorly defined. Nevertheless, the stability of this assemblage at temperatures around 600°C implies very low, if not negligible, a_{H_2O}. The calculations were performed assuming anhydrous conditions. Consequently, the pressures determined are minimum estimates.

The different geobarometric expressions applied to the metapelites assume that cordierites can be approximated to an ideal two-site mixing and either assume ideal mixing of garnet components (Holdaway & Lee, 1977; Newton & Wood, 1979; Lonker, 1981; Martignole & Sissi, 1981) or use activity–composition relation accounting for the non-ideal mixing of garnet components (Bhattacharya, 1986). The calibrations of Holdaway & Lee (1977), Lonker (1981) and Bhattacharya (1986) yield similar results in the 550–650°C temperature range which are respectively: 4.5–5.1 kbar, 4.5–5.0 kbar and 4.6–5.7 kbar (see also Fig.7a). The calibrations of Newton & Wood (1979) and Martignole & Sissi (1981) give lower estimates (3.8–4.8 kbar and 2.5–3.3 kbar respectively).

Thermobarometry on mafic assemblages

Temperatures were estimated from Grt–Opx thermometers (Harley, 1984a; K. Lal & M. Raith in Srikantappa, Raith & Ackermand 1985 and written communication, 1985). Pressures were determined from Grt–Opx–Pl–Qtz assemblages using the calibrations of Newton & Perkins (1982), Bohlen, Wall & Boettcher (1983) and Perkins & Chipera (1985), and from the Grt–Opx Al-barometer (Harley, 1984b) and the Grt–Ol–Pl barometer (Newton, 1983; Bohlen *et al.*, 1983).

Temperatures

Temperatures calculated from 20 Grt–Opx pairs with the calibration of Harley (1984a) are in the range 512–676°C, except for three extreme values (475, 720 and 723°C). The temperatures for samples IC-115 (512–638°C) and IC-115B (565–631°C) are in the same range as those for the metapelites (Fig.7). The highest estimates were obtained on the more magnesian sample IC-114A (630–723°C).

The calibration of Lal & Raith yields similar results for the samples IC–115 and IC–115B (Fig.7c and d) but much higher temperatures for sample IC-114A (>800°C; Fig.7e). Such high values could be due to the high X_{Mg} of phases because this calibration of the Grt–Opx exchange equilibrium is not applicable for compositions close to the end-members (M. Raith, written communication, 1986).

Pressures

Pressures determined from norites are consistent with those obtained from the metapelitic assemblages. Pressure estimates derived from both Grt–Opx–Pl and Grt–Ol–Pl assemblages with the calibrations of Newton & Perkins (1982), Newton (1983) and Bohlen *et al.*,(1983) are in a narrow range (3.5–6.8 kbar) The data obtained from the Grt–Opx barometer of Perkins & Chipera (1985) and from the Grt–Opx Al-barometer of Harley (1984b) are more scattered (1.0–8.7 kbar and 3.7–9.3 kbar, respectively) but consistent with the former ones. The

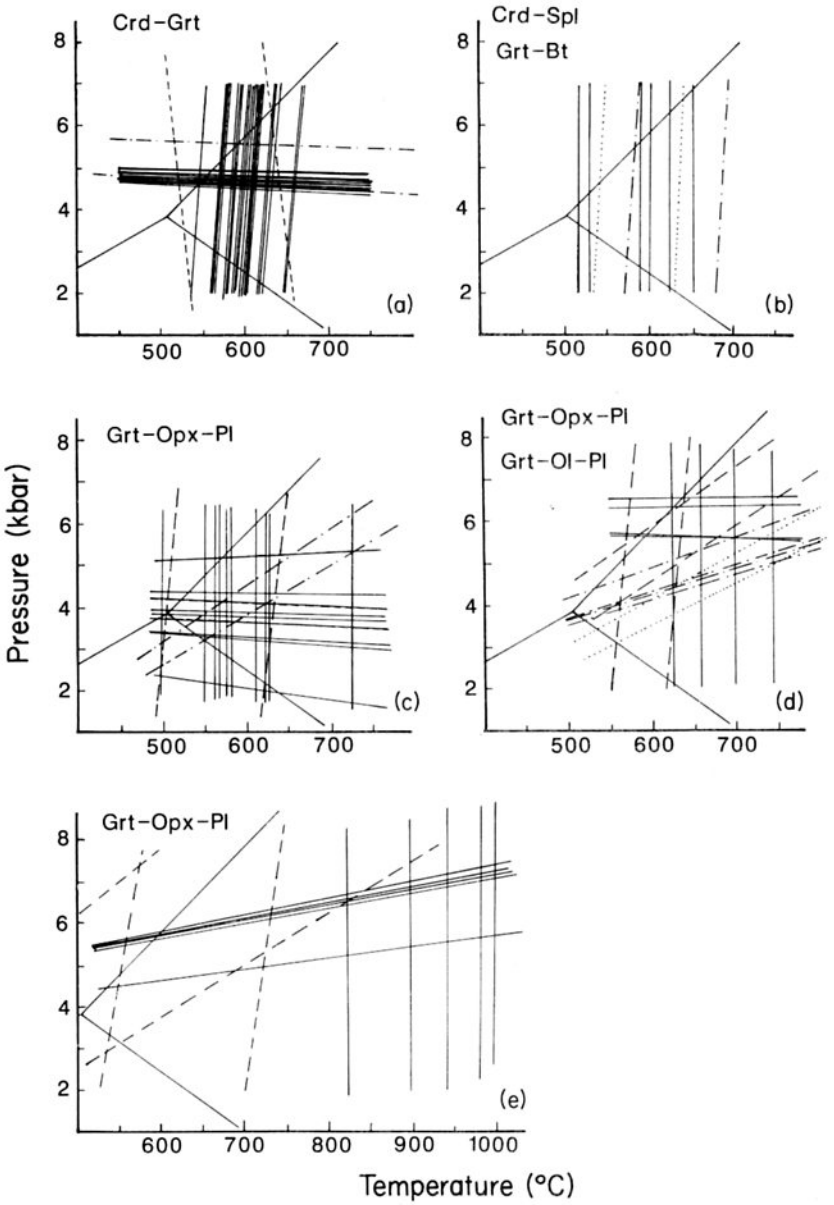

Fig. 7. Diagram showing the results of geothermobarometry. Al_2SiO_5 phase diagram from Holdaway (1971). (a) Crd–Grt thermobarometry on samples IC-15 and IB-1267. (——) *T* and *P* according to Thompson (1976) and Holdaway & Lee (1977); (---) *T* and *P* ranges according to Wells (1979) and Bhattacharya (1986). (b) Crd–Spl and Grt–Bt thermometry on samples IC-15 and IB-1267. (——) Crd–Spl thermometry (Vielzeuf, 1983); (· · · · ·) Grt–Bt thermometry according to Hodges & Spear (1982); (·–·–) Grt–Bt thermometry according to Ferry & Spear (1978). (c) Grt–Opx–Pl thermobarometry on sample IC-115. (——) *T* and *P* according to Lal & Raith (in Srikantappa *et al.* 1985) and Newton & Perkins (1982); (– – –) *T* range according to Harley (1984a); (–·–·–) $Log_{10}K$ range according to Bohlen *et al.* (1983). (d) Grt–Opx–Pl and Grt–Ol–Pl thermobarometry on sample IC-115B. *Grt–Opx–Pl*; (——) *T* and *P* according to Lal & Raith (Srikantappa *et al.*, 1985) and Newton & Perkins (1982); (– – –) *T* and $Log_{10}K$ ranges according to Harley (1984a) and Bohlen *et al.* (1983); *Grt–Ol–Pl*; (· · · ·): $Log_{10}K$ range according to Bohlen *et al.* (1983); (·–·–) *P* according to Newton (1983). (e) Grt–Opx–Pl thermobarometry on sample IC 114A. Same as (d).

Table 4. X_{Fe}^{Grt}, $\ln K_D$, and T(°C) (Thompson, 1976) for some representative zoned garnets associated with cordierite and sillimanite.

Sample number	X_{Fe}^{Grt}	$\ln K_D$	T(°C)
Small euhedral garnets (Fig. 3b)			
IC–15–3A			
rim	0.791	2.309	601
core	0.802	2.385	581
core	0.799	2.358	588
rim	0.791	2.296	605
IC–15–3B			
rim	0.791	2.260	615
core	0.796	2.273	613
Subhedral to anhedral garnets			
IC–15–2A			
rim	0.764	2.215	628
core	0.786	2.115	658
core	0.790	2.314	600
rim	0.796	2.406	576
IC–15–5B			
rim	0.791	2.210	629
core	0.773	2.073	671
IB–1267–1			
rim	0.814	2.354	589
core	0.795	2.197	633

results for the three studied samples are consistent with each other and given in Table 5.

Garnet zoning

Two types of zoning have been observed (see previous sections): (1) a zoning characterized by an increase in X_{Mg} rimward and found only in metapelites, and (2) a zoning characterized by a decrease in X_{Mg} toward the rim and observed in both metapelites and norites.

The first type is typical of the small euhedral garnets associated with sillimanite needles in cordierite (Fig.3b). In this case, the K_D values increase rimward (Table 4) therefore suggesting that this zoning can be regarded as Pan-African prograde growth zoning.

The second type corresponds to a decrease in X_{Mg} rimward. It affects the subhedral to anhedral garnet grains sometimes associated with sillimanite in metapelites, and is general in norites. This zoning is associated with a decrease in the K_D values rimward (Table 4) and might be interpreted as Pan-African retrograde zoning. However, it is difficult to explain why the large garnets would be affected by retrograde zoning but not the smallest ones. A more likely explanation is that this normal zoning corresponds either to an overgrowth of Pan-African garnet on a previous residual Eburnean garnet equilibrated at higher P,T conditions, or to a relict Eburnean retrograde zoning.

DISCUSSION

On the basis of previous structural and geochronological data, it can be demonstrated that the two-stage granulitic coronas are clearly related to a polycyclic evolution. In this respect, the discussion of Calabria (Schenk, 1984; Vielzeuf, 1984) emphasizes the necessity of careful structural observations and geochronological data to interpret these two-stage coronas.

Comparing the different thermobarometric results from both the pelitic and mafic assemblages leads us to estimate the P,T conditions of equilibration of these assemblages during the Pan-African metamorphic event at about 5 ± 1 kbar and 620 ± 50°C. Moreover, this estimate could probably represent near-climactic conditions, as suggested by the existence of prograde growth zoning in garnets from metapelites. The homogeneity of temperatures all over the IGU, irrespective of the proximity of gabbroic and dioritic bodies, precludes any significant heating effect by Pan-African intrusions. Therefore, these P,T conditions

Table 5. Range of pressures (kbar) obtained on the three samples of norites, for the 550–650°C temperature range using different calibrations: (1) Newton & Perkins (1982), (2) Bohlen *et al.* (1983), (3) Perkins & Chipera (1985), (4) Newton (1983), (5) Harley (1984)

Assemblage	Calibration	IC–115	IC–115B	IC–114A
Grt–Opx–Pl	(1)	3.5–4.5	5.8–6.5	4.0–6.0
	(2)	3.2–5.3	3.8–6.7	3.0–8.5
	(3)	6.7–9.3	7.3–9.0	3.7–5.2
Grt–Ol–Pl	(4)		3.7–5.9	
	(2)		3.0–4.7	
Grt–Opx/Al	(5)	2.6–8.7	1.6–7.9	1.0–3.1

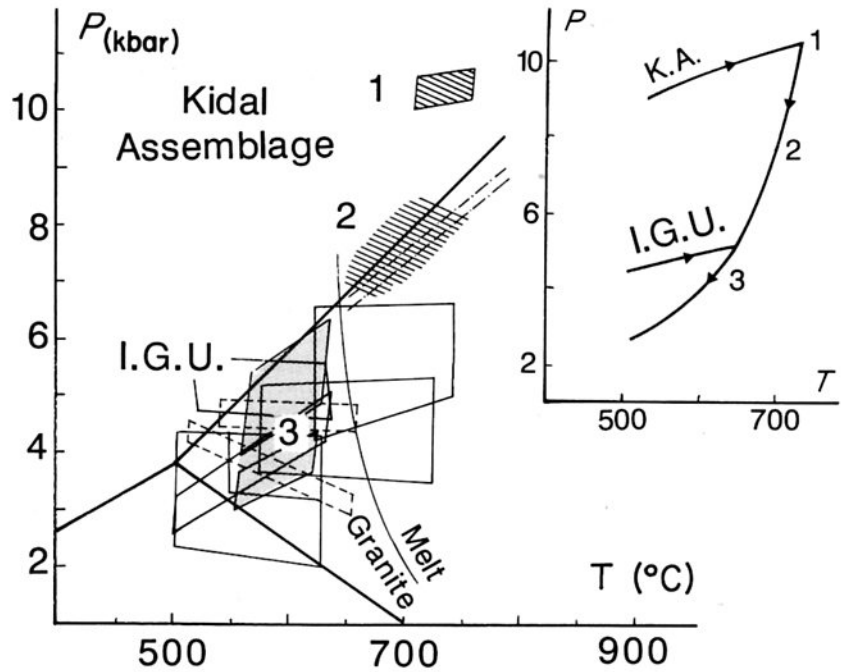

Fig. 8. Synoptic *P–T* data and interpretative *P–T–t* path for the Iforas Granulite Unit and the Kidal Assemblage during the Pan-African event. Data for the Kidal Assemblage (▨) from Champenois *et al.*, (1987). Data for the IGU (□) from Fig. 7.

1982), it appears likely that the common evol- probably reflect a rather high geothermal gradient. The close identity between the pressures estimated from norites and those estimated from metapelites clearly corroborates the hypothesis of very low water fugacities during the Pan-African metamorphic event.

The underlying Kidal Assemblage experienced a two-stage evolution during the Pan-African (Boullier, 1982; Champenois *et al.*, 1987). A paroxysmal stage in the kyanite stability field, estimated at 700±50°C and 10±1 kbar, was followed by a migmatization episode at lower pressure near to or below the kyanite – sillimanite phase transition (650 – 750°C, 7–8 kbar) and synchronous with the thrusting deformation (Fig.8). The mylonitic structures linked to this thrusting event are observed both in the Kidal gneiss assemblage and IGU. As these mylonites are coeval with the granulite facies recrystallizations (Boullier, ution of the two units began at the peak conditions recorded in the IGU.

The fact that the Iforas granulites were outcropping before the Pan-African orogeny and that the Kidal assemblage experienced higher pressures than the granulites during the Pan-African, leads us to propose the following evolution. The IGU together with its autochtonous sedimentary cover, was overthrust by Upper Proterozoic supracrustals and tectonically buried to a depth of *c.*20km, and then thrust over and attached to the Kidal Assemblage which was going up at the same time. Both units were subsequently uplifted together (Fig.8). The *P–T–t* path of these two units is very similar to those in other collisional orogens where the crust is thickened by thrusting, deduced either from thermobarometry on mineral assemblages (e.g. Bucher-Nurminen & Droop, 1983; Barbey *et al.*, 1984; Hollister & Crawford, 1986) or from calculation models (Albarède, 1976; England & Thompson, 1984). These results confirm the tectonic interpretation of this segment of the Trans-Saharan Pan-African belt previously proposed by Boullier *et al.*, (1978), Wright (1979), Davison (1980) and Champenois *et al.* (1987). However it should be noted that in contrast with the case-study of Hollister & Crawford (1986) in the Coast Mountains of British Columbia, the structurally lowest unit of the Adrar des Iforas (Kidal

Assemblage) was metamorphosed at higher pressures that the overlying IGU

Another interesting and important feature is that the retrogression of the Iforas granulites during the Eburnean metamorphic evolution occurred under almost anhydrous conditions, leading only to the growth of a little biotite in metapelites or biotite and hornblende in mafic rocks. It appears likely that this anhydrous Eburnean retrogression (preservation of high X_{CO_2} in the fluid phase) is a prerequisite condition for the development of a new granulite facies metamorphism during the Pan-African orogeny. During this event, X_{H_2O} probably increased moderately after the thrusting of the granulites upon the Kidal Assemblage where dehydration reactions occurred. However, the percolation of fluid from below was restricted to the sole of the nappe and to localized vertical shear zones (characterized by intense deformation and recrystallization of hornblende and biotite) which acted also as weakness zones for intrusion of plutonic bodies. The fact that these rocks remained dry may also account for the local reaction control and limited recrystallization during the Pan-African.

Thus, the Pan-African reworking of the IGU was not complete and left some large blocks where the whole Eburnean and Pan-African history can be reconstructed.

ACKNOWLEDGEMENTS

One of the authors (A.M.B.) thanks the Direction Nationale de la Géologie et des Mines de Bamako (Mali) for providing facilities for field work. Thanks are due to R.Caby for providing some samples. Reviews by J.R. Kiénast, J. Kornprobst, M. Pichavant, M. Raith and D. Vielzeuf improved the first manuscript. Critical comments by two anonymous referees were very helpful and much appreciated. C. Devey kindly overhauled the English. This project was partly supported by CNRS (ATP Paragenèses et Associations Minérales, 1982). CRPG contribution number 731.

REFERENCES

Albaréde, F., 1976. Thermal models of post-tectonic decompression as examplified by the Haut–Allier granulites (Massif Central, France). *Bulletin de la Société Géologique de France*, **XVIII**, 1023–1032.

Barbey, P., Convert J., Moreau, B., Capdevila, R. & Hameurt, J., 1984. Petrogenesis and evolution of an early Proterozoic collisional orogenic belt-the granulite belt of Lapland and the Belomorides (Fennoscandia). *Bulletin of the Geological Society of Finland*, **56**, 161–188.

Bertrand, J.M., Michard, A., Carpena, J., Boullier, A.M., Dautel, D. & Ploquin, A., 1984. Pan-African granitic and related rocks in the Iforas granulites (Mali). Structure, geochemistry and geochronology. In *African Geology* (ed. Klerkx, J. & Michot, J).pp.147–165. MRAC, Tervuren.

Bhattacharya, A., 1986. Some geobarometers involving cordierite in the $FeO–Al_2O_3–SiO_2–(\pm H_2O)$ system: refinements, thermodynamic calibration and application in granulite facies rocks. *Contributions to Mineralogy and Petrology*, **94**, 387–394.

Bingen, B., Demaiffe, D. & Delhal, J., 1984. Petrologic and geothermobarometric investigations in the Kasai gabbro-norite complex and associated metadoleritic dykes (Zaire). *Bulletin de Minéralogie*, **107**, 665–682.

Black, R., Caby, R., Moussine-Pouchkine, A., Bayer, R., Bertrand, J.M.L., Boullier, A.M., Fabre, J. & Lesquer, A., 1979. Evidence for late Precambrian plate tectonics in West Africa. *Nature*, **278**, 223–227.

Bohlen, S.R., Wall, V.J. & Boettcher, A.L., 1983. Experimental investigations and application of garnet granulite equilibria. *Contributions to Mineralogy and Petrology*, **83**, 52–61.

Boullier, A.M., 1979, Charriage et défromations de l'Unité Granulitique des Iforas au cours de l'orogénèse Pan-Africaine. *Revue de Géographie physique et de Géologie dynamique*, **21**, 377–382.

Boullier, A.M., 1982. Etude structurale du centre de l'Adrar des Iforas (Mali). Mylonites et tectogénèse. *Unpubl. thesis, INPL Nancy*.

Boullier, A.M., 1986. Sense of shear and displacement estimates in the Abeibara–Rharous late Pan-African shear zone (Adrar des Iforas, Mali). *Journal of Structural Geology*, **8**, 47–58.

Boullier, A.M., Davison, I., Bertrand, J.M. & Coward, M., 1978. L'unité granulitique des Iforas: une nappe de socle d'âge Pan-Africain précoce. *Bulletin de la Société Geologique France*, **XX**. 877–882.

Bucher-Nurminen, K. & Droop, G., 1983. The metamorphic evolution of garnet–cordierite–sillimanite gneisses of the Gruf Complex, Eastern Pennine Alps. *Contributions to Mineralogy and Petrology*, **84**, 215–227.

Caby, R., Bertrand, J.M. & Black, R. 1981. Pan-African closure and continental collision in the Hoggar-Iforas segment, Central Sahara. In *Precambrian Plate Tectonics* (ed. Kröner, A.), pp.407–434. Elsevier, Amsterdam.

Cahen, L., Snelling, N.J., Delhal, J. & Vail, J.R., 1984 *The Geochronology and Evolution of Africa*. Clarendon Press, Oxford.

Champenois, M., Boullier, A.M., Sautter, V., Wright, L.I. & Barbey, P., 1987. Tectonometamorphic evolution of the gneissic Kidal Assemblage related to the Pan-African thrust tectonics (Adrar des Iforas, Mali). *Journal of African Earth Sciences*,**6**, 19–28.

Davison, I., 1980. A tectonic, petrographical and geochronological study of a Pan-African belt in the Adrar des Iforas and Gourma (Mali). *Unpubl. PhD thesis, University of Leeds, Centre Géologique et Géophysique de Montpellier*.

Ellis, D.J. & Green, D.H., 1985. Garnet-forming reactions in mafic granulites from Enderby Land, Antarctica — implications for geothermometry and geobarometry. *Journal of Petrology*, **26**, 633–662.

England, P.C. & Thompson, A.B., 1984. Pressure–temperature–time paths of regional metamorphism. I — Heat transfer during the evolution of regions of thickened continental crust. *Journal of Petrology*, **25**, 894–928.

Ferry, J.M. & Spear, F.S., 1978. Experimental calibration of the partitioning of Fe and Mg between biotite and garnet. *Contributions to Mineralogy and Petrology*, **66**, 113–117

Garde, A.A., Glassley, W.E. & Nutman, A.P., 1984. Two-stage corona growth during Precambrian granulite facies metamorphism of Smithson Bjerge, north-west Greenland. *Journal of Metamorphic Geology*, **2**, 237–247.

Harley, S.L., 1984a. An experimental study of the partitioning of Fe and Mg between garnet and orthopyroxene. *Contributions to Mineralogy and Petrology*, **86**, 359–373.

Harley, S.L., 1984b. The solubility of alumina in orthopyroxene coexisting with garnet in $FeO–MgO–Al_2O_3–SiO_2$ and $CaO–FeO–MgO–Al_2O_3–SiO_2$. *Journal of Petrology*, **25**, 665–696.

Harley, S.L., 1985. Garnet–orthopyroxene bearing granulites from Enderby Land, Antarctica: metamorphic pressure–temperature–time evolution of the Archean Napier Complex. *Journal of Petrology*, **26**, 819–856.

Henoc, J. & Tong, M., 1978. Automatisation de la microsonde. *Journal de Microscopie et de Spectroscopie Electronique*, **3**, 247–254.

Hodges, K.V. & Spear, F.S., 1982. Geothermometry, geobarometry and the Al_2O_5 triple point at Mt. Moosilauke, New Hampshire. *American Mineralogist*, **67**, 1118–1134.

Holdaway, M.J., 1971. Stability of andalusite and the aluminium silicate phase diagram. *American Journal of Science*, **271**, 97–131.

Holdaway, M.J.& Lee, S.M., 1977. Fe-Mg cordierite stability in high-grade pelitic rocks based on experimental, theoretical and natural observations. *Contributions to Mineralogy and Petrology*, **63**, 175–198.

Hollister, L.S. & Crawford, M.L., 1986. Melt-enhanced deformation: a major tectonic process. *Geology*, **14**, 558–561.

Lancelot, J.R., Boullier, A.M., Maluski, H. & Ducrot, J., 1983. Deformation and related radiochronology in a late Pan-African mylonitic shear zone. *Contributions to Mineralogy and Petrology*, **82**, 312–326.

Lonker, S.W., 1981. The *P–T–X* relations of the cordierite–garnet–sillimanite–quartz equilibrium. *American Journal of Science*, **281** 1056–1090.

Martignole, J. & Sissi, J.C., 1981. Cordierite–garnet–H_2O equilibrium: a geological thermometer, barometer and water fugacity indicator. *Contributions to Mineralogy and Petrology*, **77**, 38–46.

McLelland, J.M. & Whitney, P.R., 1980. Compositional controls on spinel clouding and garnet formation in plagioclase of olivine metagabbros, Adirondack mountains, New York. *Contributions to Mineralogy and Petrology*, **73**, 243–251.

Montel, J.M., Weber, C. & Pichavant, M., 1986. Biotite – sillimanite – spinel assemblages in high-grade metamorphic rocks: occurrences, chemographic analysis and thermobarometric interest. *Bulletin de Minéralogie*, **109**, 555–573.

Newton, R.C., 1983. Geobarometry of high-grade metamorphic rocks. In *Studies in Metamorphism and Metasomatism*. (ed. Greenwood H.J.) *American Journal of Science*, **283A**, 1–28.

Newton, R.C. & Perkins, D., III, 1982. Thermodynamic calibration of geobarometers based on the assemblages garnet – plagioclase – orthopyroxene (clinopyroxene) – quartz. *American Mineralogist*, **67**, 203–222.

Newton, R.C. & Wood, B.J., 1979. Thermodynamics of water in cordierite and some petrologic consequences of cordiertie as a hydrous phase. *Contributions to Mineralogy and Petrology*, **68**, 391–405.

Perkins D. & Chipera, S.J., 1985. Garnet–orthopyroxene–plagioclase–quartz barometry: refinement and application to the English River subprovince and the Minnesota River Valley. *Contributions to Mineralogy and Petrology*, **89**, 69–80.

Pigage L.C. & Greenwood H.J., 1979. Internally consistent estimates of pressure and temperature: The staurolite problem. *American Journal of Science*, **282**, 943–969.

Richardson, S.W., 1968. Staurolite stability in a part of the system Fe–Al–Si–O–H. *Journal of Petrology*, **9**, 467–488.

Schenk, V., 1984. Petrology of felsic granulites, metapelites, metabasics, ultramafics and metacarbonates from Southern Calabria (Italy). Prograde metamorphism, uplift and cooling of a former lower crust. *Journal of Petrology*, **25**, 255–298.

Srikantappa, C., Raith, M. & Ackermand, D., 1985. High-grade regional metamorphism of ultramafic and mafic rocks from the Archaean Sargur terrane, Karnataka, South India. *Precambrian Research*, **30**, 189–219.

Thompson, A.B., 1976. Mineral reactions in pelitic rocks: II — calculation of some *P–T–X* (Fe–Mg) phase relations. *American Journal of Science*, **276**, 401–424.

Vielzeuf, 1983. the spinel and quartz associations in high-grade xenoliths from Tallante (SE-Spain) and their potential use in geothermometry and barometry. *Contributions to Mineralogy and Petrology*, **82**, 301–311.

Vielzeuf, 1984. Relations de phases dans le faciés granulite et implications géodynamiques. L'exemple des granulites des Pyrénées. *Unpubl. thesis, University of Clermont.*

Wells, P.R.A., 1979. Chemical and thermal evolution of Archaean sialic crust, Southern West Greenland. *Journal of Petrology*, **20**, 187–226.

Wright, L., 1979. The pattern of movement and deformation during the Pan-African, in the Adrar des Iforas. *10th Colloquium of African Geology*, Montpellier, Abstract, 77.

Received 19 May 1987; revision accepted 2 October 1987.